



Published in final edited form as:

Biochemistry. 2008 December 2; 47(48): 12869–12877. doi:10.1021/bi801779d.

Resonance Raman Interrogation of the Consequences of Heme Rotational Disorder in Myoglobin and its Ligated Derivatives

Freeborn Rwere, Piotr J. Mak, and James R. Kincaid*

Chemistry Department, Marquette University, Milwaukee, WI 53233

Abstract

Resonance Raman spectroscopy is employed to characterize heme site structural changes arising from conformational heterogeneity in deoxyMb and ligated derivatives; i.e., the ferrous CO (MbCO) and ferric cyanide (MbCN) complexes. The spectra for the reversed forms of these derivatives have been extracted from the spectra of reconstituted samples. Dramatic changes in the low frequency spectra are observed, where newly observed RR modes of the reversed forms are assigned using protohemes that are selectively deuterated at the four methyl groups or at the four methine carbons. Interestingly, while substantial changes in the disposition of the peripheral vinyl and propionate groups can be inferred from the dramatic spectral shifts, the bonds to the internal histidyl imidazole ligand and those of the Fe-CO and Fe-CN fragments are not significantly affected by the heme rotation, as judged by lack of significant shifts in the $\nu(\text{Fe-N}_{\text{His}})$, $\nu(\text{Fe-C})$ and $\nu(\text{C-O})$ modes. In fact, the apparent lack of an effect on these key vibrational parameters of the Fe-N_{His}, Fe-CO and Fe-CN fragments is entirely consistent with previously reported equilibrium and kinetic studies that document virtually identical functional properties for the native and reversed forms.

Conformational heterogeneity involving rotational disorder of the heme about the α - γ meso axis (Figure 1) in native and reconstituted myoglobins was first studied by NMR spectroscopy and circular dichroism (CD) spectroscopy in the 1980's.¹⁻⁸ This conformational heterogeneity has been found to occur not only in the reconstituted metMb form,³ but also in the native deoxy² and ligated forms; i.e., MbCO.³ At equilibrium, the reversed conformation still persists in very small amounts for aquo-metMb (~4% for HH Mb²⁴ and ~8% for SW Mb³) and deoxy Mb, MbCO and metMb-CN (~8% for SW Mb)^{2,3} while for the recently discovered met neuroglobin (metNgb) an ~70/30 ratio has been reported.⁸

Most of these studies focused only on the *detection* of the reversed orientation and the effects of temperature, pH, spin states or heme peripheral substituents on the extent and kinetics of heme reorientation, the NMR studies detecting and assigning only the shifted resonances of the heme methyl protons.³ In later NMR relaxation studies, however, the structural consequences of heme orientation were investigated by analyzing the distance between the heme iron and protons of the Ile FG5 C _{γ} H and Phe CD1 C _{γ} H side chains of sperm whale Mb (SW Mb).^{9,10} These studies showed that the heme is slightly displaced away from Ile FG5 C _{γ} H in the reversed form. Though apparently displaced within the heme pocket, recent studies employing the so-called normal coordinate structural decomposition methods suggest that the protein matrices of both the native and reversed forms induce similar types of distortions on heme macrocyclic core.¹¹

*To whom correspondence should be addressed: tel, (414) 288 3539; fax, (414) 288 7066; e-mail, james.kincaid@marquette.edu.

SUPPORTING INFORMATION AVAILABLE The RR spectra of samples containing sulfate, difference spectra of native and reversed forms of proto and d12 deoxyMb, high frequency RR spectra of native and reversed forms of deoxyMb and MbCO are available free of charge via Internet at <http://pubs.scs.org>.

It has been shown that reversal of the heme orientation can change certain functional properties of *some* heme proteins.^{9-10,12-17} For example, the Bohr effect of *Chironomus* hemoglobin,¹² the heme reduction potential of cytochrome *b*₅¹³ and the affinity and degree of cooperativity in dioxygen binding by HbA¹⁴ have been reported to depend on heme orientation. In the specific case of myoglobin, though early work¹⁵ had indicated that the reversed form of deoxyMb has a 10-fold higher oxygen affinity than the native form, later reports conclusively showed that both the O₂ and CO affinities of the reversed form are essentially the same as those for the native form.^{16,17} While no significant differences in ligand affinities of the two forms are observed, Yamamoto et al. showed that the exchange rate of the N_εH proton of the E7 distal histidine in the reversed form of sperm whale metMb-CN is larger by a factor of 3-5 as compared to the native, while the exchange rates of the *proximal* His F8 N_εH protons were essentially equal for the native and reversed forms and further documented only small differences in the rates of autoxidation of the oxy complex and azide affinity of the metMb derivative.⁹

Resonance Raman spectroscopy has been used as an important tool for the study of heme proteins giving detailed structural information on the heme macrocycle through certain low frequency and high frequency modes. The oxidation state and the spin state of the heme can be documented through the so-called “marker bands” in the high frequency region.¹⁸⁻²⁰ In addition, subtle changes in the interaction of the heme iron with both endogeneous^{21,22} and exogeneous ligands^{23,24} are monitored by isotopically sensitive low frequency modes. Furthermore, the peripheral group dispositions of the “propionate” and “vinyl” bending mode are useful to document orientation dependent changes in the active site protein-heme interactions. In fact, earlier work on metMb²⁵ demonstrated that the spectrum of the reversed form can be extracted from the freshly reconstituted samples and some of the orientation-dependent heme modes of metMb have already been assigned using isotopically labeled protohemes.²⁵ Thus, prompted by results of the NMR and ligand binding studies, which seem to indicate active site structural changes that are apparently rather functionally innocuous, the present Resonance Raman investigations of the native and reversed forms have been undertaken to effectively interrogate the key Fe-N_{His} linkage to the proximal histidine and the status of the Fe-CO and Fe-CN fragments of the adducts with exogenous ligands.

The results of this current work show that significant differences between reversed and native forms are seen in the peripheral group dispositions as evidenced by frequency shifts and intensity changes of so called “propionate” and “vinyl” bending modes. However, the analyses of the acquired RR spectra show that the position of the $\nu(\text{Fe-N}_{\text{His}})$ mode did not change in the reversed deoxy form and that the modes associated with Fe-XY fragments of the CO and cyanide adducts exhibit insignificant changes between the native and reversed forms, results entirely consistent with the known lack of changes in the ligand binding properties of the rotational isomers.

EXPERIMENTAL

Materials

Protoporphyrin IX dimethyl ester (PPIXDME) and Fe(III)-protoporphyrin IX chloride (protoheme) were purchased from Frontier Science Porphyrin Products (Logan, UT). Myoglobin from horse heart (HH Mb), essentially all in the oxidized (metMb) form, was purchased from Sigma-Aldrich (Milwaukee, WI) as a lyophilized powder and was used without further purification. Deuterated dimethylsulfoxide (99.9 % ²H, DMSO-d₆) and deuterated methanol (99.0 % ²H, CH₃OD), were purchased from Cambridge Isotope Laboratories (Andover, MA). Finally, tetrabutylammonium hydroxide (TBAOH) (1 M solution in methanol), anhydrous pyridine, anhydrous acetonitrile, anhydrous tetrahydrofuran, anhydrous

hexane, anhydrous heptane, anhydrous dichloromethane and diethyl ether were purchased from Sigma-Aldrich (Milwaukee, WI).

Synthesis of Selectively Deuterated Protohemes

Deuterium substitution of the four methine carbons, designated as d4-protoheme and syntheses of 1,3-(C²H₃)₂-protoheme (1,3-d6-protoheme) and 1,3,5,8-(C²H₃)₄-protoheme (d12-protoheme) were accomplished using previously published procedures.²⁶⁻²⁹ The deuterated protohemes were crystallized from THF/heptane mixtures.²⁶⁻²⁹ Thin layer chromatograms (TLC), pyridine hemochromogen electronic absorption spectra and ¹H NMR studies were done to check the purity of the sample and the extent of deuteration.²⁹⁻³³ The ¹H NMR spectrum of d4-protoheme showed that the methine protons were deuterated to an extent of 95%. The ¹H NMR spectrum of 1,3-d6-protoheme revealed that the 1,3 methyl groups were deuterated to the extent of ~98 %, while the 5 and 8 methyl groups remained practically not deuterated (less than 10 %). The corresponding spectrum of d12-protoheme showed almost 100% deuteration of 1,3-CH₃ and ~93 % for the 5 and 8 methyl groups.

Protein Preparation

Apomyoglobin (apoMb) was obtained from met myoglobin solution using the acid-butanone method.^{34,35} The UV-Vis spectrum of the apoMb solution was measured and its concentration was calculated, using $\epsilon^{280\text{nm}} = 15.9 \text{ cm}^{-1}\text{mM}^{-1}$;³⁵ the residual heme content was 0.03%. Reconstitution of apoMb, in 25 mM phosphate buffer at pH 6.4, was carried out by adding 0.9 equivalents of protoheme (or a given deuterated analogue), which had been dissolved in a minimum amount (2 drops) of 0.1 M NaOH solution and then diluted 10 times with chilled deionized water, over a 5 minute period; during this addition, the pH of the solution was maintained at 6.4 by adding either 0.1 M HCl or 0.1 M NaOH solution. Any precipitate formed during the reconstitution was immediately removed by centrifugation for 5 minutes. At precisely 20 minutes after the reconstitution step was initiated, the samples were converted to new forms; i.e., by adding dithionite to generate deoxyMb or KCN to generate the metMb-CN. Inasmuch as it has been previously established that the deoxyMb and metMb-CN forms undergo reorientation at very slow rates,²⁻⁴ these conversions effectively halt the reorientation equilibration. Thus, the samples studied in this work are referred to as “20-minute” samples to indicate that reorientation had been allowed to proceed for 20 minutes before locking in the extent of disorder.

Specifically, the samples of deoxyMb were prepared by reduction with 2 equivalents of sodium dithionite immediately before the RR spectrum was collected noting that for these deoxy samples, the solution had been flushed with Argon gas for 10 minutes after centrifugation was completed. The samples of reconstituted MbCO were prepared from separate deoxyMb samples prepared in a similar manner, by saturating with CO gas for 10 minutes prior to acquiring the RR spectrum. In order to prepare metMb-CN adducts, the pH of reconstituted samples was adjusted to 8.0 at the 20 minute point and kept at this value while 10 equivalents of KCN was added as a 1.0 M solution.

Resonance Raman Measurements

Resonance Raman spectra were acquired using a Spex 1269 spectrometer equipped with an Andor Newton EMCCD detector (Model DU971, Andor Technologies). Excitation at 406.7 nm (krypton ion laser, Coherent Innova 100-K3) was used to acquire the RR spectra for metMb samples and 413.1 nm for the carbon-monooxy adducts. The RR spectra were collected using back scattering (180°) geometry. The spectra of the carbon-monooxy adducts were acquired using low power (less than 1.5 mW) in order to minimize photo dissociation of CO from the heme to the extent that the non-ligated deoxy form did not contribute to the observed RR spectrum, as judged by absence of the 1356 cm⁻¹ band.³⁶ Resonance Raman spectra of the

deoxy form were acquired by excitation at 441.6 nm (He-Cd laser, Liconix model 4240NB). Power at the sample was maintained at ~3 mW. All RR measurements were performed at room temperature in spinning NMR tubes (WG-5 ECONOMY, Wilmad). The concentration of the heme-incorporated protein was ~0.3 mM for all of the reconstituted samples studied here. The total acquisition time for each of the forms of Mb under study (i.e., deoxyMb, MbCO and metMb-CN) was 30 minutes per spectrum.

The RR spectra for the reversed forms were extracted according to the published procedure, using sodium sulfate as an internal frequency and intensity (I_{983}) standard.²⁵ Briefly, as was previously shown for metMb,²⁵ graphical analysis of the spectra (Grams Software; Galactic Industries, Salem, NH) showed that the intensity of the mode at 545 cm^{-1} remains virtually constant for the native and reversed forms; i.e., the I_{545}/I_{983} ratios in the 20-minute and native spectra are identical (Supporting Information, Figure S1). It has also been shown that the intensity of the 370 cm^{-1} mode in the spectrum of the deoxyMb sample, 30 minutes after reconstitution, is decreased by 42% relative to that of the 545 cm^{-1} mode. This percentage corresponds well to the previously reported value measured by NMR for deoxyMb soon after reconstitution; i.e., the percentage of the reversed form was calculated to be 40-45%.² This observation served as a basis to assume that the 370 cm^{-1} band is absent (i.e., shifted) in the spectrum of the reversed form, permitting the extraction of the reversed form spectrum by simple subtraction of the native form spectrum from that of the 30-min sample such that the 370 cm^{-1} band was completely cancelled. A similar procedure was applied for extraction of the reversed form spectra for the CO and CN⁻ ligated Mbs; e.g., the deconvolution of 20-minute spectrum of MbCO at 379 cm^{-1} as well as 20-minute spectrum of metMb-CN at 375 cm^{-1} showed intensity decreases of those modes by approximately 40% as compared to corresponding spectra of native CO and CN⁻ forms, consistent with the fractional disorder determined by NMR data for metMb-CN² and MbCO³, data in the latter study consisting of ring current shifts.

RESULTS AND DISCUSSION

The RR data reported in this work reveal the existence of the heme in two orientations, with the native orientation dominating at equilibrium. The assignments of the new low frequency bands are based on shifts observed using selectively labeled hemes; 1,3-d6, d12 and d4-protohemes. The 1,3-d6-protoheme, possessing two deuterated methyl groups at positions 1 and 3, allows identification of vibrational modes associated with pyrroles I and II.^{25,28} The d12-protoheme, having all four methyl groups deuterated, yields shifts of vibrational modes associated with the III and IV pyrrole rings, which bear the 5- and 8-methyl and both propionate groups, as well as the those for I and II pyrrole rings that bear the 1- and 3-methyl and both vinyl groups.^{25,28} The d4-protoheme, having all methine protons replaced with deuterium, exhibits shifts of modes associated with the heme macrocycle, the most substantial shifts being observed for out-of-plane (oop) modes, especially the γ_6 mode.^{28,41}

A. Deoxy Mb

1. Assignments—Figure 2 shows the observed low frequency RR spectra of native deoxyMb (trace A) and the protoheme-reconstituted deoxyMb at 20 minutes (trace B). The spectra in Figure 2 (traces A and B) are normalized using the γ_{21} band at 545 cm^{-1} , since the intensity of this mode remains constant in the 20-minute reconstituted and native spectra, relative to the intensity of the sulfate internal standard band (not shown). Trace C shows the extracted spectrum of the reversed form of deoxyMb, obtained by using the procedure explained in the Experimental section. As was observed in an earlier RR study of rotational disorder for metMb,²⁵ a set of new features are observed in the extracted spectrum of the reversed form of deoxyMb; these appear at 251 cm^{-1} , 298 cm^{-1} , 335 cm^{-1} , 360 cm^{-1} , 388 cm^{-1} , 420 cm^{-1} and 480 cm^{-1} , the strongest of which can be discerned in trace B. As in the case of the reversed

metMb,²⁵ in order to assign these low frequency modes in reversed deoxyMb, reconstitution was carried out using the selectively deuterated protohemes mentioned above, with the extracted spectra for these labeled reversed forms, together with the spectrum of native deoxyMb, being shown in Figure 3. Table 1 summarizes the assignments of the RR modes of deoxyMb and the ligated Mbs studied here along with those of metMb reported previously.²⁵

Before proceeding to a discussion of the structural implications of these data, it is necessary to provide points of clarification regarding the “descriptions” of assignments. While the features located near 370-380 cm^{-1} and those between 400-450 cm^{-1} in the RR spectra of many heme proteins are commonly referred to as “propionate bending” and “vinyl bending” modes, respectively, that fact that both of these features are also shifted quite substantially upon deuteration of the ring methyl groups verifies the fact that these are actually pyrrole ring deformations, involving motions of the porphyrin core atoms and methyl substituents as well as the vinyl or propionate fragments, the main point being that the frequencies and intensities of these complex modes are apparently sensitive to the disposition of these peripheral fragments that interact with the surrounding protein. Thus, given the complexity of the modes in this low frequency region, it may be the case that more than two modes might be considered to have contributions from “vinyl bending” or “propionate bending” motions and, indeed, the appearance of three “vinyl bending” modes has been reported in several papers dealing with different heme proteins.^{37,38}

2. Structural Implications—The rather striking changes observed in the low frequency region of the RR spectra induced by the heme rotation presumably reflect alterations in the protein-heme interactions between the two forms, although it is noted that the key linkage between the heme and the protein, the $\nu(\text{Fe}-\text{N}_{\text{His}})$ stretching mode, is apparently not substantially altered, being found in Figure 3 at 220 cm^{-1} for both the native (trace A) and reversed (Trace B) forms. One particularly noticeable observation in trace B is the apparent disappearance of the ν_9 seen at 240 cm^{-1} in the spectrum of the native form (trace A). Although a new weak feature is seen at 251 cm^{-1} in trace B, it exhibits much greater sensitivity to heme methyl group deuteration than does the ν_9 mode of the native form (i.e., 11 cm^{-1} vs 2 cm^{-1} for 1,3-d6-protoheme and 14 vs 7 cm^{-1} for d12-protoheme) and is therefore not reasonably assignable to the ν_9 for the reversed form. Actually, this disappearance of the ν_9 mode in trace B is entirely consistent with observations made for mutant forms of deoxyMb by Friedman and coworkers, who noted a strong correlation between the behaviors of the ν_9 mode and the propionate bending mode seen near 370 cm^{-1} .³⁹ These authors employed mutants that disrupt the hydrogen bonding interactions between the heme-7-propionate and amino acids on the proximal side that apparently leads to a more flexible or extended propionate fragment exposed to solvent, a structural change that caused the propionate mode to shift down by 1-8 cm^{-1} for different mutants. Most interestingly, these authors also showed that this spectral response of the propionate mode was associated with corresponding decreases in the frequency of the ν_9 mode, shifting it to the extent that it became unclear whether the mode had blended smoothly into the $\nu(\text{Fe}-\text{N}_{\text{His}})$ or disappeared completely.³⁹

These present results strongly support these earlier observations when taking into consideration the behavior observed here for this so-called propionate bending mode (designated as III,IV in Figure 3). Thus, in trace A this III,IV mode occurs at 370 cm^{-1} and the ν_9 mode is relatively strong, whereas in trace B the propionate bending mode has shifted down to 360 cm^{-1} and the ν_9 mode has virtually disappeared. While the earlier work provided no definitive insight as to whether or not this mode had shifted in frequency to coalesce with the $\nu(\text{Fe}-\text{N}_{\text{His}})$ or so diminished in intensity as to be undetectable, the present set of data provides a clear cut answer to this question. Thus, as shown in Supporting Information (Figure S2), subtraction of trace B from trace A, shows only a positive peak at 240 cm^{-1} and an extremely weak negative feature at $\sim 220 \text{ cm}^{-1}$, which could be due to either a shifted ν_9 or to a very slight difference in intensities

of the $\nu(\text{Fe-N}_{\text{His}})$ modes. Plotting a corresponding difference trace for the native and reversed forms of the d12-protoheme analogues shows, however, that this residual 220 cm^{-1} peak does not shift by 7 cm^{-1} as does the ν_9 mode that shows a positive peak at 233 cm^{-1} , as expected; i.e., apparently the intensity of the ν_9 mode for the reversed form has diminished to an undetectable level.

It is also noted that in the spectrum of reversed deoxyMb the γ_6 and ν_8 modes have collapsed into one slightly asymmetric feature, the weaker γ_6 mode reappearing at a virtually unshifted frequency in trace D as the stronger ν_8 mode shifts down to 326 cm^{-1} for the d12-protoheme analogue. Such behavior is again quite consistent with predictions made by Friedman and coworkers,³⁹ who showed that in the set of mutant proteins they studied, a downshift of the propionate bending mode is accompanied by a merging of the γ_6 and ν_8 modes.

To the extent that such arguments are valid, the shift of the propionate bending mode to 360 cm^{-1} indicates that the hydrogen bond strength to relatively fixed amino acid residues has been substantially weakened in the reversed form, possibly allowing the propionate groups to become more exposed to solvent. The crystal structure of HH Mb shows that a hydrogen bonding network involving Leu89, Ser92, His93, His97 and the heme-7-propionate on the proximal side is responsible for stabilizing the heme in the protein matrix while the heme-6-propionate only forms a hydrogen bond with Lys45 on the distal side.⁴⁰ The RR spectra of myoglobin only show one “propionate bending” mode in the low frequency region. While the data presented here cannot distinguish whether or not this mode contains contributions from only the 7-propionate or both of them, the fact that proximal side mutations in the earlier work generated the type of changes seen here, might imply that the disposition of only this 7-propionate group affects the low frequency RR spectrum; however, only studies with protohemes selectively labeled at either the 6- or 7-propionate groups could unambiguously answer this question.

In the region $400\text{--}450\text{ cm}^{-1}$ in the spectrum of native deoxyMb form, there appear the so-called “vinyl bending” modes, which actually contain major contributions from $\delta(\text{C-C}_\beta\text{-CH}_3)$ bending motions, as discussed above. Based on the work with specifically deuterated vinyl groups,⁴¹⁻⁴³ the 405 cm^{-1} feature is assigned to deformations of pyrrole II, involving motions of the 4-vinyl group, while the higher frequency (436 cm^{-1}) feature is assigned to a deformation mode of pyrrole I (the 2-vinyl bending mode). In the spectrum of the reversed form, the new modes found at 388 cm^{-1} and 420 cm^{-1} are assigned to these “vinyl bending” modes, based on a set of isotopic shifts similar to those observed for the native form. At this point it is not possible to associate these with either the 2- or 4-vinyl groups, since such assignment can be secured only by selective isotopic labeling of specific vinyl groups. Regardless of assignments to specific vinyl group contributions, however, it is generally accepted that a lower frequency vinyl bending mode (e.g., 405 cm^{-1}) is associated with a higher degree of planarity of the vinyl and pyrrole, while a higher frequency mode (436 cm^{-1}) is associated with more out-of-plane configuration.^{38,44}

The high frequency region was also monitored in order to attempt to secure evidence for changes in the $\nu(\text{C}=\text{C})$ vinyl stretching modes, whose frequencies have been reliably related to vinyl group planarity with respect to the porphyrin core, by Smulevich and coworkers.^{42, 45} As is illustrated in the difference spectra given in Supporting Information (Figure S3), the native form exhibits only one $\nu(\text{C}=\text{C})$ stretch at 1618 cm^{-1} , while the reversed form possesses an *additional* mode at 1632 cm^{-1} , a value consistent with conversion of a portion of the more planar vinyl groups to more out-of-plane orientations. It is noted that the difference plot also reveals another interesting feature that indicates that the so-called ν_2 mode, which is associated with the $\nu(\text{C}_\beta\text{-C}_\beta)$ stretching mode, exhibits some corresponding changes; i.e., the intensity

near 1564 cm^{-1} decreases for the native form, while that at 1553 cm^{-1} increases in the reversed form, such changes being consistent with decreased conjugation in the reversed form.

B. Ligated Forms

1. Assignments—The spectra of the native and 20-minute reconstituted MbCO forms are shown in Figure 4 along with the extracted spectrum of the reversed form of MbCO, while Figure 5 illustrates the extracted spectra for the reversed forms obtained for proto, 1,3-d6, d12 and d4-protoheme reconstituted MbCO. As expected, the extracted spectra for the reversed forms show the existence of new low frequency heme modes, many of which have frequencies different from those of the native MbCO form, but virtually no significant difference in the frequencies of the $\nu(\text{Fe-CO})$ mode. These data are collected in Table 1, which shows that there is good correspondence, in terms of their relative frequencies and isotopic sensitivity, between the modes observed and assigned for deoxyMb and MbCO, as well as those observed for metMb in an earlier work.²⁵ As is shown in Supporting Information (Figure S.4), the only changes in the high frequency RR spectrum of the reversed form, relative to that of the native form, is the appearance of a new band seen at 1629 cm^{-1} , that is attributable to a second $\nu(\text{C=C})$ vinyl stretch, consistent with the appearance of the two “vinyl bending” modes seen at 392 and 427 cm^{-1} . Further, it is noted that (native - reversed form) difference spectrum given in Supporting Information for the $1900 - 2000\text{ cm}^{-1}$ region (Figure S.5), in which occur the $\nu(\text{C-O})$ stretching modes, shows no evidence for shifts of these modes, the lack of shifts in this region reinforcing the point that the Fe-C-O fragment of the reversed form is not significantly perturbed from that of the native form.

In the spectrum of reversed MbCO there is a new feature appearing at 356 cm^{-1} that is not observed in the spectrum of native MbCO. The isotopic shift of this mode is consistent with a ν_{50} assignment, based on a comparison with reference compounds.⁴⁶⁻⁴⁹ Similarly, the weak feature at 366 cm^{-1} , being only slightly sensitive to 1,3-d6 and d12-protoheme (blending in with other shifted modes in these isotopomers), but more sensitive to d4-protoheme (shifting 19 cm^{-1} to 347 cm^{-1}), is assigned to the γ_6 mode, which is also not observed in the spectrum of the native form. The frequency of this mode is quite variable in the RR spectra of heme proteins, being observed near 340 cm^{-1} for metMb^{25,41} and deoxyMb (Table 1), but up to 367 cm^{-1} for substrate-bound forms of cytochrome P450.^{37,50} While this mode is found at only 350 cm^{-1} in the RR spectra of CO derivatives of HbA,⁵¹ it is found at 362 cm^{-1} in the spectra of ferrous CO adducts of cytochrome c peroxidase⁴² and near 360 cm^{-1} for model compounds,⁴⁶⁻⁴⁹ these latter frequencies being quite consistent with the 366 cm^{-1} value observed here.

Figure 6 illustrates the low frequency RR spectra of the native and 20-minute reconstituted forms of metMb-CN, as well as the extracted spectrum of the reversed form of metMb-CN. While the band at 453 cm^{-1} is clearly attributable to the $\nu(\text{Fe-CN})$ stretching mode, based on well documented shifts observed when employing isotopically labeled KCN,²³ it has also been shown that the internal modes of the Fe-C-N fragment can couple with low frequency heme modes leading to isotopic sensitivity in features observed at 257 cm^{-1} , 302 cm^{-1} , 385 cm^{-1} , 404 cm^{-1} , 425 cm^{-1} and 440 cm^{-1} .⁵² The feature appearing at 375 cm^{-1} for native metMb-CN is assigned to propionate bending vibrations (i.e., pyrroles III and IV), while the band at 410 cm^{-1} is assigned to 4-vinyl bending vibrations from pyrrole II, based on work with hemes bearing selectively deuterated vinyl groups.⁴¹⁻⁴³ In addition, the band at 440 cm^{-1} , which showed some CN-isotopic sensitivity,⁵² also contains some contributions from (2-vinyl bending) pyrrole I deformation.⁴¹ In the reversed form, the propionate bending mode is found as a weak feature appearing at 370 cm^{-1} , while only one broad vinyl mode is found at 425 cm^{-1} ; actually, given the complications of interpretation that arise in this region because of the apparent coupling of heme modes and internal modes of the Fe-C-N fragment, it is not possible to clarify the assignments of the 405 and 425 cm^{-1} features, without more extensive labeling

experiments, although it does seem clear that there is no new observable “vinyl bending” mode near 390 cm^{-1} , but there seems to be enhanced intensity near 425 cm^{-1} that would be consistent with appearance of a new vinyl bending mode at this frequency, similar to those seen for all three other derivatives (i.e., the deoxy, met- and CO derivatives).

2. Structural Implications—While the RR spectral data obtained here for the ligated derivatives of reversed form of HH Mb indicate some significant perturbations of the protein-heme interactions, there is little effect on the FeXY fragments, just as there is little effect of the rotation on the Fe-N_{his} linkage of the deoxy derivative, as shown in Part A, above. Thus, not only do the $\nu(\text{Fe-C})$ stretching and $\delta(\text{FeCO})$ bending modes fail to exhibit significant shifts ($< 2\text{ cm}^{-1}$ in the *extracted* spectra), but the more structure-sensitive $\nu(\text{C-O})$ modes observed between 1920 and 1970 cm^{-1} in the spectrum of the reversed MbCO form are clearly unshifted as judged by the lack of difference bands appearing in the inset of Figure S.5.

This lack of substantial effects of the rotation on distal side H-bonding interactions with bound exogenous ligands implied by the data on the Fe-C-O fragment is reinforced by corresponding data acquired here for the metMb-CN sample, inasmuch as the frequencies of the Fe-C-N fragment have been shown to be sensitive to such interactions. Thus, comparing NMR data for cyanide adducts of heme proteins and model compounds, Fujii and Yoshida showed that certain parameters are sensitive to H-bonding by distal pocket donors and further showed that in the H64A mutant of SW Mb, the H-bonding interaction is lost.⁵³ Significantly, a corresponding RR study of the cyanide adducts of SW Mb and this H64A mutant documented a 7 cm^{-1} shift to lower frequency for the $\nu(\text{Fe-CN})$ mode of the mutant.⁵⁴ Thus, the lack of any shift in the $\nu(\text{Fe-CN})$ mode in the reversed form of HH metMb-CN implies that any H-bonding changes that might occur lead to insignificant changes in the strength of this Fe-CN linkage.

The $370\text{--}450\text{ cm}^{-1}$ region that contains modes that involve the movement of propionate and vinyl substituents show that the propionate modes of MbCO and metMb-CN, appearing near 375 cm^{-1} in the native forms, are shifted down by only $4\text{--}5\text{ cm}^{-1}$ from those of native forms, these shifts being only about 50% of those seen for the deoxyMb and metMb samples, implying that the disposition of the propionate groups of *ligated* forms are less perturbed by the heme rotation. In the reversed form of MbCO, new “vinyl bending” modes are found at 392 cm^{-1} and 427 cm^{-1} while only a single new mode is observed at 425 cm^{-1} for metMb-CN, which apparently overlaps a weak unassigned mode observed at this frequency of the native form. As in the cases of the deoxy and met-derivatives, two “vinyl bending” modes, observed near $400\text{--}410\text{ cm}^{-1}$ and near $430\text{--}440\text{ cm}^{-1}$ for the native form, are shifted in such a way upon rotation to generate two new “vinyl bending” modes, with a relatively weak feature observed $\sim 390\text{ cm}^{-1}$ and a substantially stronger one at $\sim 425\text{ cm}^{-1}$. As was mentioned above, in the absence of data acquired for disordered forms bearing specifically labeled vinyl groups, it is not possible to attribute the vinyl bending modes to particular vinyl groups; however, based on the fact that the two new modes still yield one lower frequency vinyl bending mode and one relatively high frequency mode near 425 cm^{-1} it seems most reasonable to suggest that the rotation does not lead to dramatically different distributions of in-plane and out-of-plane vinyl groups.

C. Relationship to Functional Properties

While the RR data clearly demonstrate that the rotation of the heme about the $\alpha\text{--}\gamma$ axis in various derivatives of HH myoglobin causes substantial changes in the disposition of vinyl and propionate groups with respect to the heme plane or surrounding protein residues, the rotation apparently has minimal effects on the strength of the linkages between the heme iron and the endogenous histidyl imidazole or exogenous CO or CN ligands. These spectral data then imply that while the reorientation of the heme might affect some inherent heme properties, such as the reduction potential, it is would be expected to have minimal effects on binding of exogenous

ligands. In fact, this implication is entirely consistent with previously reported ligand binding studies. Thus, kinetic studies with SW Mb showed that the rates of CO recombination after photolysis were identical for the major and the minor forms.^{16,17} The authors concluded that SW Mb exhibits essentially the same CO affinity in both forms. The rates of O₂ combination with deoxyMb following laser photolysis of the MbCO derivative in the presence of O₂ were studied by Light et al. and Ajoula et al.^{16,17} The calculated bimolecular rate constant for the reconstituted samples were identical to those of the native protein for SW Mb implying that the O₂ affinities are basically the same for the two forms, all results being consistent with the RR data acquired here.

Supplementary Material

Refer to Web version on PubMed Central for supplementary material.

Acknowledgements

This work was supported by National Institutes of Health (DK 35153 to JRK), as well as the Pfltschinger Habermann Fund and Way-Klingler award from Marquette University.

Abbreviations

Mb, myoglobin; HH Mb, horse heart myoglobin; SW Mb, sperm whale myoglobin; HbA, human hemoglobin; oop, out-of-plane; TBAOH, tetrabutylammonium hydroxide; THF, tetrahydrofuran.

REFERENCES

1. La Mar, GN.; Satterlee, JD.; De Ropp, JS. Nuclear magnetic resonance of hemoproteins. In: Kadish, KM.; Smith, KM.; Guillard, R., editors. *Porphyrin Handbook*. Vol. Vol 5. Academic Press; New York: 2000. p. 185-298.
2. La Mar GN, Davis NL, Parish DW, Smith KM. Heme orientational disorder in reconstituted and native sperm whale myoglobin. Proton nuclear magnetic resonance characterizations by heme methyl deuterium labeling in the met-cyano protein. *J. Mol. Biol* 1983;168:887–896. [PubMed: 6887254]
3. Jue T, Krishnamoorthi R, La Mar GN. Proton NMR study of the mechanism of the heme-apoprotein reaction for myoglobin. *J. Am. Chem. Soc* 1983;105:5701–5703.
4. La Mar GN, Toi Hiroo, Krishnamoorthi R. Proton NMR investigation of the rate and mechanism of heme rotation in sperm whale myoglobin: evidence for intramolecular reorientation about a heme two-fold axis. *J. Am. Chem. Soc* 1984;106:6395–6401.
5. La Mar GN, Yamamoto Y, Jue T, Smith KM, Pandey RK. Proton NMR characterization of metastable and equilibrium heme orientational heterogeneity in reconstituted and native human hemoglobin. *Biochemistry* 1985;24:3826–3831. [PubMed: 4052368]
6. Bellelli A, Foon R, Ascoli F, Brunori M. Heme disorder in two myoglobins: comparison of reorientation rate. *Biochem. J* 1987;246:787–789. [PubMed: 3689333]
7. La Mar GN, Pande U, Hauksson JB, Pandey RK, Smith KM. Proton nuclear magnetic resonance investigation of the mechanism of the reconstitution of myoglobin that leads to metastable heme orientational disorder. *J. Am. Chem. Soc* 1989;111:485–491.
8. Du W, Syvitski R, Dewilde S, Moens L, La Mar GN. Solution ¹H NMR characterization of equilibrium heme orientational disorder with functional consequences in mouse neuroglobin. *J. Am. Chem. Soc* 2003;125:8080–8081. [PubMed: 12837059]
9. Yamamoto Y, Nakashima T, Kawano E, Chujo R. ¹H-NMR investigation of the influence of the heme orientation on functional properties of myoglobin. *Biochim. Biophys. Acta* 1998;388:349–362. [PubMed: 9858764]
10. Yamamoto Y, Kawano E. Functional and structural consequences of heme orientational disorder in myoglobin. *J. Inorg. Biochem* 1997;67:119.

11. Kiefl C, Sreerama N, Haddad R, Sun L, Jentzen W, Lu Y, Qiu Y, Shelnutt JA, Woody RW. Heme Distortions in Sperm-Whale Carbonmonoxy Myoglobin: Correlations between Rotational Strengths and Heme Distortions in MD-Generated Structures. *J. Am. Chem. Soc* 2002;124:3385–3394. [PubMed: 11916424]
12. Gersonde K, Sick H, Overkamp M, Smith KM, Parish DW. Bohr effect in monomeric insect hemoglobins controlled by oxygen off-rate and modulated by heme-rotational disorder. *Euro. J. Biochem* 1986;157:393–404.
13. Walker FA, Emrick D, Rivera JE, Hanquet BJ, Buttlare DH. Effect of heme orientation on the reduction potential of cytochrome b5. *J. Am. Chem. Soc* 1988;110:6234–6240.
14. Nagai M, Nagai Y, Aki Y, Imai K, Wada Y, Nagatomo S, Yamamoto Y. Effect of Reversed Heme Orientation on Circular Dichroism and Cooperative Oxygen Binding of Human Adult Hemoglobin. *Biochemistry* 2008;47:517–525. [PubMed: 18085800]
15. Livingston DJ, Davis NL, La Mar GN, Brown WD. Influence of heme orientation on oxygen affinity in native sperm whale myoglobin. *J. Am. Chem. Soc* 1984;106:3025–3026.
16. Light WR, Rohlfis RJ, Palmer G, Olson JS. Functional effects of heme orientational disorder in sperm whale myoglobin. *J. Biol Chem* 1987;262:46–52. [PubMed: 3793732]
17. Aojula HS, Wilson MT, Morrison IG. Functional consequences of haem orientational disorder in sperm-whale and yellow-fin-tuna myoglobins. *Biochem. J* 1987;243:205–210. [PubMed: 3606571]
18. Spiro TG. Resonance Raman spectroscopy as a probe of heme protein structure and dynamics. *Advances in Protein Chemistry* 1985;37:111–159. [PubMed: 2998161]
19. Kincaid, JR. Resonance Raman spectra of heme proteins and model compounds. In: Kadish, KM.; Smith, KM.; Guillard, R., editors. *Porphyrin Handbook*. Vol. Vol 7. Academic Press; New York: 2000. p. 225-291.
20. Spiro TG, Streckas TC. Resonance Raman spectra of heme proteins. Effects of oxidation and spin state. *J. Am. Chem. Soc* 1974;96:338–345. [PubMed: 4361043]
21. Kitagawa, T. The heme protein structure and the iron histidine stretching mode. In: Spiro, TG., editor. *Biological Applications of Raman Spectroscopy*. Vol. Vol. 3. Wiley & Sons; New York: 1988. p. 97-131.
22. Rousseau DG, Rousseau DL. Hydrogen bonding of iron-coordinated histidine in heme proteins. *J. Struc. Biol* 1992;109:13–17.
23. Yu, N-T.; Kerr, EA. Vibrational modes of coordinated CO, CN⁻ and NO. In: Spiro, TG., editor. *Biological Applications of Raman Spectroscopy*. Vol. Vol. 3. Wiley & Sons; New York: 1988. p. 39-95.
24. Wang, J.; Caughey, WS.; Rousseau, DL. Resonance Raman scattering: a probe of heme protein-bound nitric oxide. In: Feelisch, M.; Stamler, J., editors. *Methods in Nitric Oxide Research*. John Wiley; New York: 1996. p. 427-454.
25. Rwere F, Mak PJ, Kincaid JR. The impact of altered protein-heme interactions on the resonance Raman spectra of heme proteins. *Studies of heme rotational disorder. Biopolymers* 2008;89:179–186. [PubMed: 18008322]
26. Godziela GM, Kramer SK, Goff HM. Rapid base-catalyzed deuterium exchange at the ring-adjacent methyl and methylene positions of octaalkyl and natural-derivative porphyrins and metalloporphyrins. *Inorg. Chem* 1986;25:4286–4288.
27. Podstawka E, Kincaid JR, Proniewicz LM. Resonance Raman studies of selectively labelled hemoglobin tetramers. *J. Mol. Struc* 2001;596:157–162.
28. Mak PJ, Podstawka E, Kincaid JR, Proniewicz LM. Effects of systematic peripheral group deuteration on the low-frequency resonance Raman spectra of myoglobin derivatives. *Biopolymers* 2004;75:217–228. [PubMed: 15378481]
29. Podstawka E, Mak PJ, Kincaid JR, Proniewicz LM. Low frequency resonance Raman spectra of isolated α and β subunits of hemoglobin and their deuterated analogues. *Biopolymers* 2006;83:455–466. [PubMed: 16845667]
30. Fuhrhop, J-H.; Smith, KM. Laboratory methods. In: Smith, KM., editor. *Porphyrin and Metalloporphyrins*. Elsevier; North Holland, Amsterdam: 1975. p. 757-869.
31. Barbush M, Dixon DW. Use of the nuclear Overhauser effect to assign proton NMR resonances in a low-spin paramagnetic hemin. *Biochem. Biophys. Res. Comm* 1985;129:70–75. [PubMed: 4004883]

32. Buchler, JW. Synthesis and Properties of metalloporphyrins. In: Dolphin, D., editor. *The Porphyrins; Structure and Synthesis, Part A*. Vol. Vol. 1. Academic Press; New York: 1978. p. 389-483.
33. DiNello RK, Dolphin DH. Analytical chromatography of hemins on silica gel. *Anal. Biochem* 1975;64:444–449. [PubMed: 165744]
34. Wittenberg, JB.; Wittenberg, BA. Preparation of myoglobins. In: Antonini, E.; Bernardi, LR.; Chiancone, E., editors. *Methods in Enzymology*. Vol. Vol 76. Academic Press; New York: 1981. p. 29-42.
35. Ascoli, F.; Fanelli, MRR.; Antonini, E. Preparation and properties of apohemoglobin and reconstituted hemoglobins. In: Antonini, E.; Bernardi, LR.; Chiancone, E., editors. *Methods in Enzymology*. Vol. Vol 76. Academic Press; New York: 1981. p. 72-87.
36. Rousseau DL, Argade PV. Metastable photoproducts from carbon monoxide myoglobin. *Proc. Natl. Acad. Sci. U.S.A* 1986;83:1310–1314. [PubMed: 3456590]
37. Mak PJ, Kaluka D, Manyumwa M. Ed. Zhang H, Deng T, Kincaid JR. Defining resonance Raman spectral responses to substrate binding by cytochrome P450 from *Pseudomonas putida*. *Biopolymers* 2008;89:1045–1053. [PubMed: 18655143]
38. Chen Z, Ost TWB, Schelvis JPM. Phe393 Mutants of Cytochrome P450 BM3 with Modified Heme Redox Potentials Have Altered Heme Vinyl and Propionate Conformations. *Biochemistry* 2004;43:1798–1808. [PubMed: 14967021]
39. Peterson ES, Friedman JM, Chien EYT, Sligar SG. Functional Implications of the Proximal Hydrogen-Bonding Network in Myoglobin: A Resonance Raman and Kinetic Study of Leu89, Ser92, His97, and F-Helix Swap Mutants. *Biochemistry* 1998;37:12301–12319. [PubMed: 9724545]
40. Evans SV, Brayer GD. High-resolution study of the three-dimensional structure of horse heart metmyoglobin. *J. Mol. Biol* 1990;213:885–897. [PubMed: 2359126]
41. Hu S, Smith KM, Spiro TG. Assignment of protoheme resonance Raman spectrum by heme labeling in myoglobin. *J. Am. Chem. Soc* 1996;118:12638–12646.
42. Smulevich G, Hu S, Rodgers KR, Goodin DB, Smith KM, Spiro TG. Heme-protein interactions in cytochrome c peroxidase revealed by site-directed mutagenesis and resonance Raman spectra of isotopically labeled hemes. *Biospectroscopy* 1996;2:365–376.
43. Uchida K, Susai Y, Hirotani E, Kimura T, Yoneya T, Takeuchi H, Harada I. 4-Vinyl and 2,4-divinyl deuteration effects on the low frequency resonance Raman bands of myoglobin: correlation with the structure of vinyl group. *J. Biochem* 1988;103:979–985. [PubMed: 3170524]
44. Kalsbeck WA, Ghosh A, Pandey RK, Smith KM, Bocian DF. Determinants of the Vinyl Stretching Frequency in Protoporphyrins. Implications for Cofactor-Protein Interactions in Heme Proteins. *J. Am. Chem. Soc* 1995;117:10959–10968.
45. Marzocchi MP, Smulevich G. Relationship between heme vinyl conformation and the protein matrix in peroxidases. *J. Raman Spectrosc* 2003;34:725–736.
46. Li X-Y, Czernuszewicz RS, Kincaid JR, Spiro TG. Consistent porphyrin force field. 3. Out-of-plane modes in the resonance Raman spectra of planar and ruffled nickel octaethylporphyrin. *J. Am. Chem. Soc* 1989;111:7012–7023.
47. Li X-Y, Czernuszewicz RS, Kincaid JR, Stein P, Spiro TG. Consistent porphyrin force field. 2. Nickel octaethylporphyrin skeletal and substituent mode assignments from nitrogen-15, meso-d4, and methylene-d16 Raman and infrared isotope shifts. *J. Phys. Chem* 1990;94:47–61.
48. Kitagawa T, Abe M, Ogoshi H. Resonance Raman spectra of octaethylporphyrinatonicel(II) and meso-deuterated and nitrogen-15 and substituted derivatives. I. Observation and assignments of nonfundamental Raman lines. *J. Chem. Phys* 1978;69:4516–4525.
49. Abe M, Kitagawa T, Kyogoku Y. Resonance Raman spectra of octaethylporphyrinatonicel(II) and meso-deuterated and nitrogen-15 substituted derivatives. II. A normal coordinate analysis. *J. Chem. Phys* 1978;69:4526–4534.
50. Deng TJ, Proniewicz LM, Kincaid JR, Yeom H, Macdonald IDG, Sligar SG. Resonance Raman Studies of Cytochrome P450BM3 and Its Complexes with Exogenous Ligands. *Biochemistry* 1999;38:13699–13706. [PubMed: 10521277]
51. Jayaraman V, Spiro TG. Structural evolution of the heme group during the allosteric transition in hemoglobin: insights from resonance Raman spectra of isotopically labeled heme. *Biospectroscopy* 1996;2:311–316.

52. Hirota S, Ogura T, Shinzawa-Itoh K, Yoshikawa S, Kitagawa T. Observation of Multiple CN-Isotope-Sensitive Raman Bands for CN Adducts of Hemoglobin, Myoglobin, and Cytochrome c Oxidase: Evidence for Vibrational Coupling between the Fe-C-N Bending and Porphyrin In-Plane Modes. *J. Phys. Chem* 1996;100:15274–15279.
53. Fujii H, Yoshida T. ^{13}C and ^{15}N NMR Studies of Iron-Bound Cyanides of Heme Proteins and Related Model Complexes: Sensitive Probe for Detecting Hydrogen-bonding Interactions at the Proximal and Distal Sides. *Inorg. Chem* 2006;45:6816–6827. [PubMed: 16903738]
54. Zhao X, Vyas K, Nguyen BD, Rajarathnam K, La Mar GN, Li T, Phillips GN Jr, Eich RF, Olson JS, Ling J, Bocian DF. A double mutant of sperm whale myoglobin mimics the structure and function of elephant myoglobin. *J. Biol. Chem* 1995;270:20763–20774. [PubMed: 7657659]

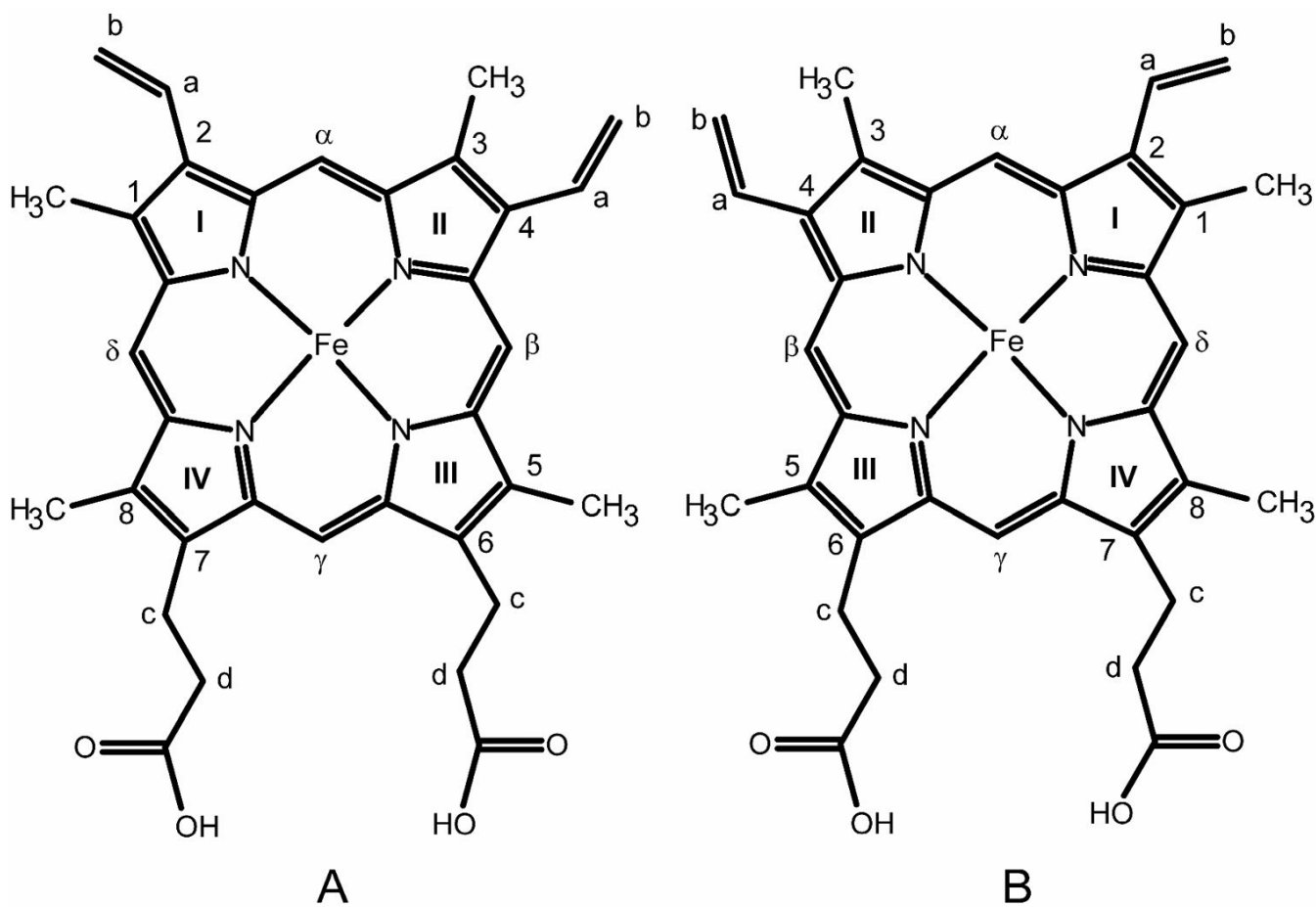


Figure 1. Structure and labeling of Fe(III) protoporphyrin IX, native orientation, (A); and reversed orientation, (B).

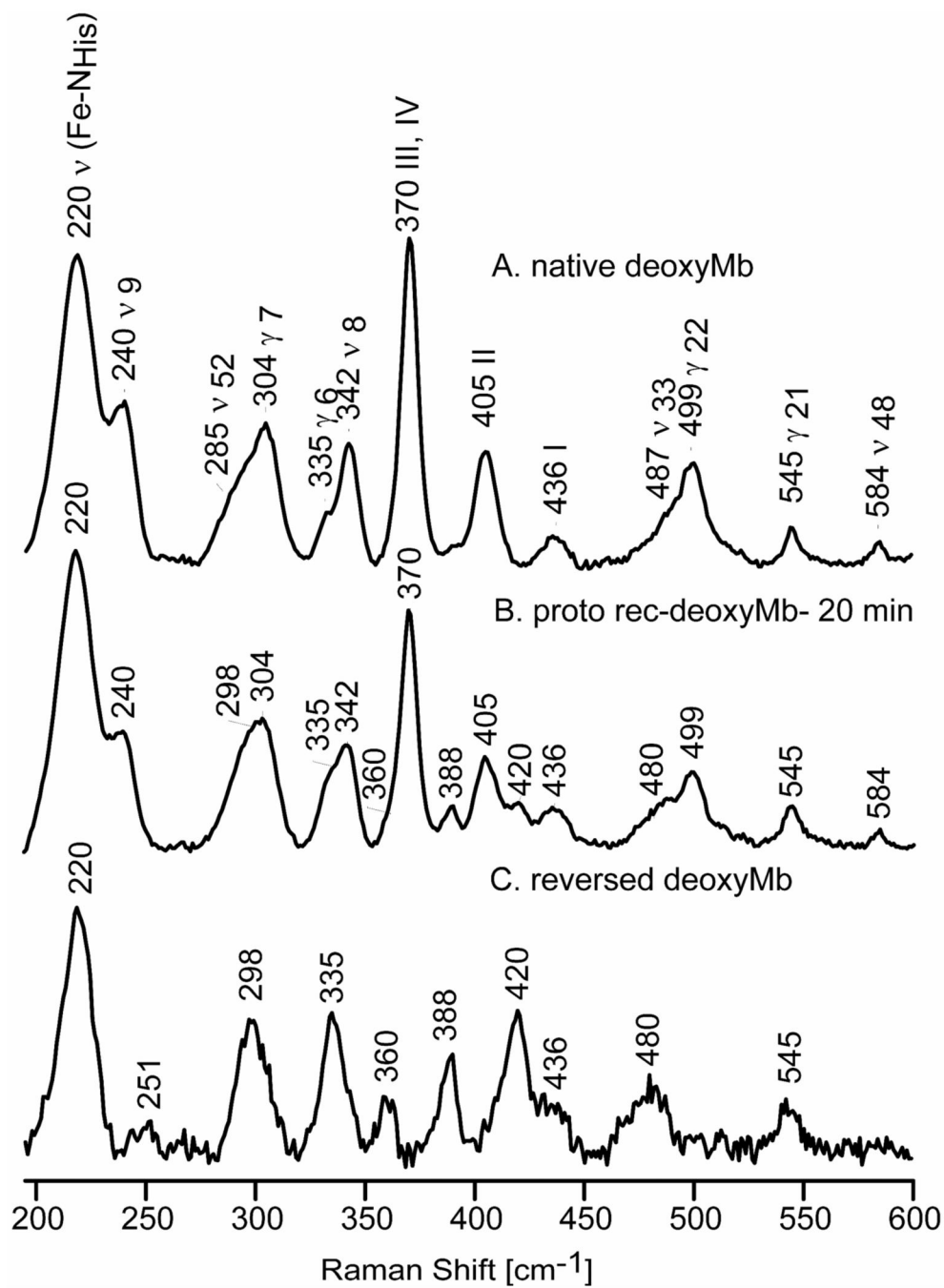


Figure 2. Low frequency RR spectra of native deoxyMb, (A); 20-minutes reconstituted deoxyMb, (B); and reversed deoxyMb, (C).

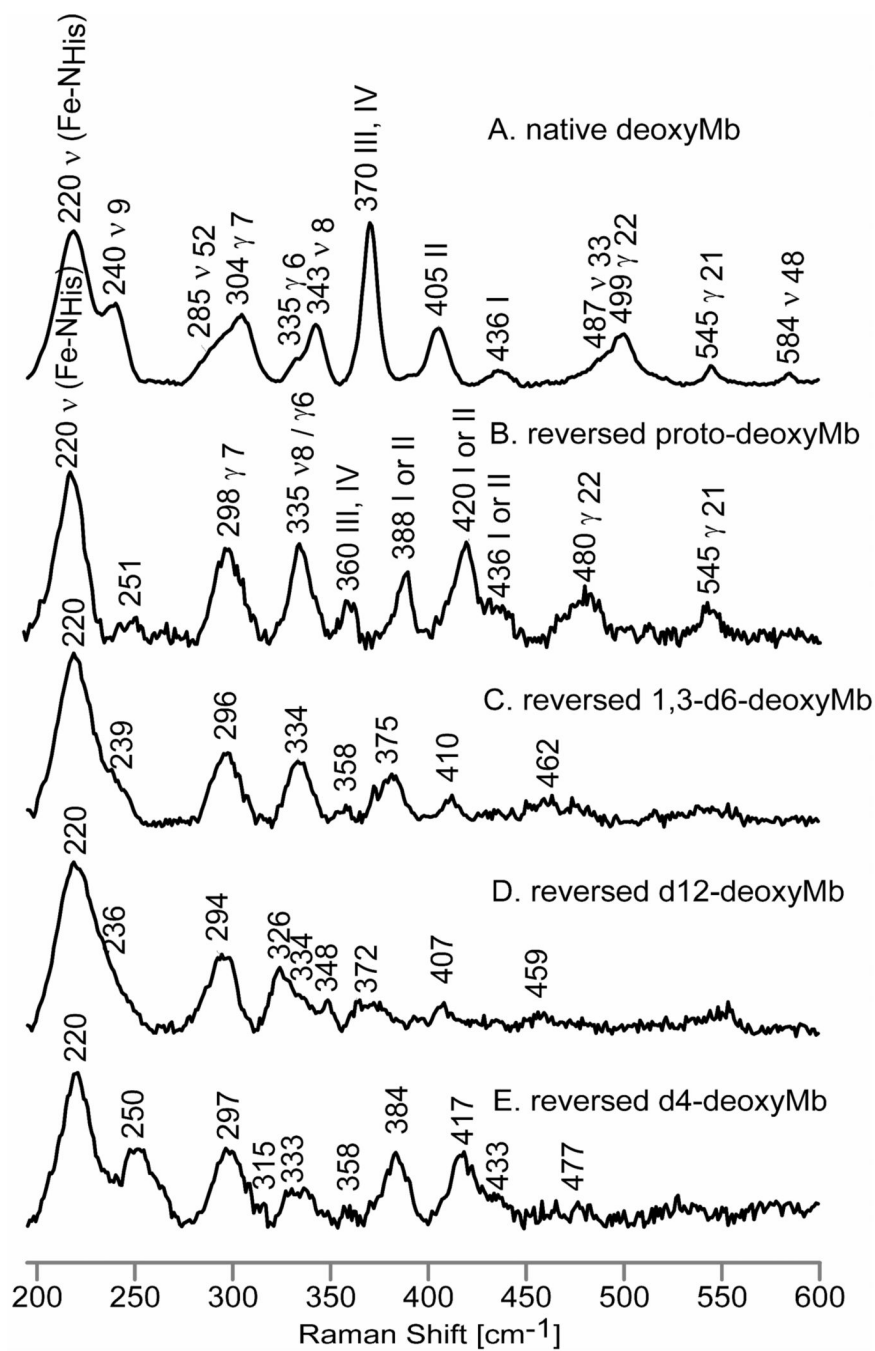


Figure 3. Low frequency RR spectra of native deoxyMb, (A); reversed proto-deoxyMb, (B); reversed 1,3-d6-deoxyMb, (C); reversed d12-deoxyMb, (D) and reversed d4-deoxyMb, (E).

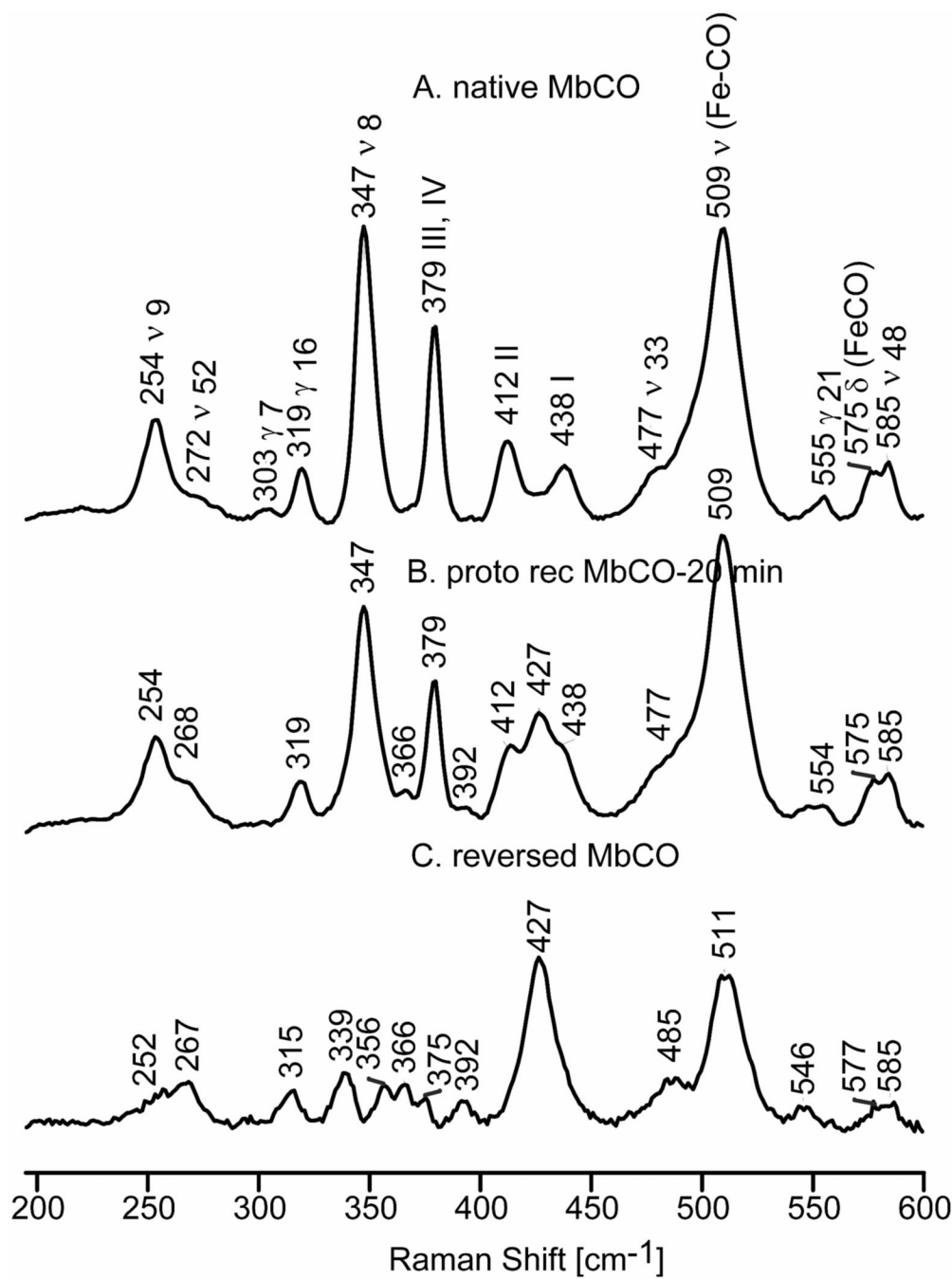


Figure 4. Low frequency RR spectra of native MbCO, (A); proto reconstituted MbCO at 20 minutes, (B) and reversed MbCO, (C).

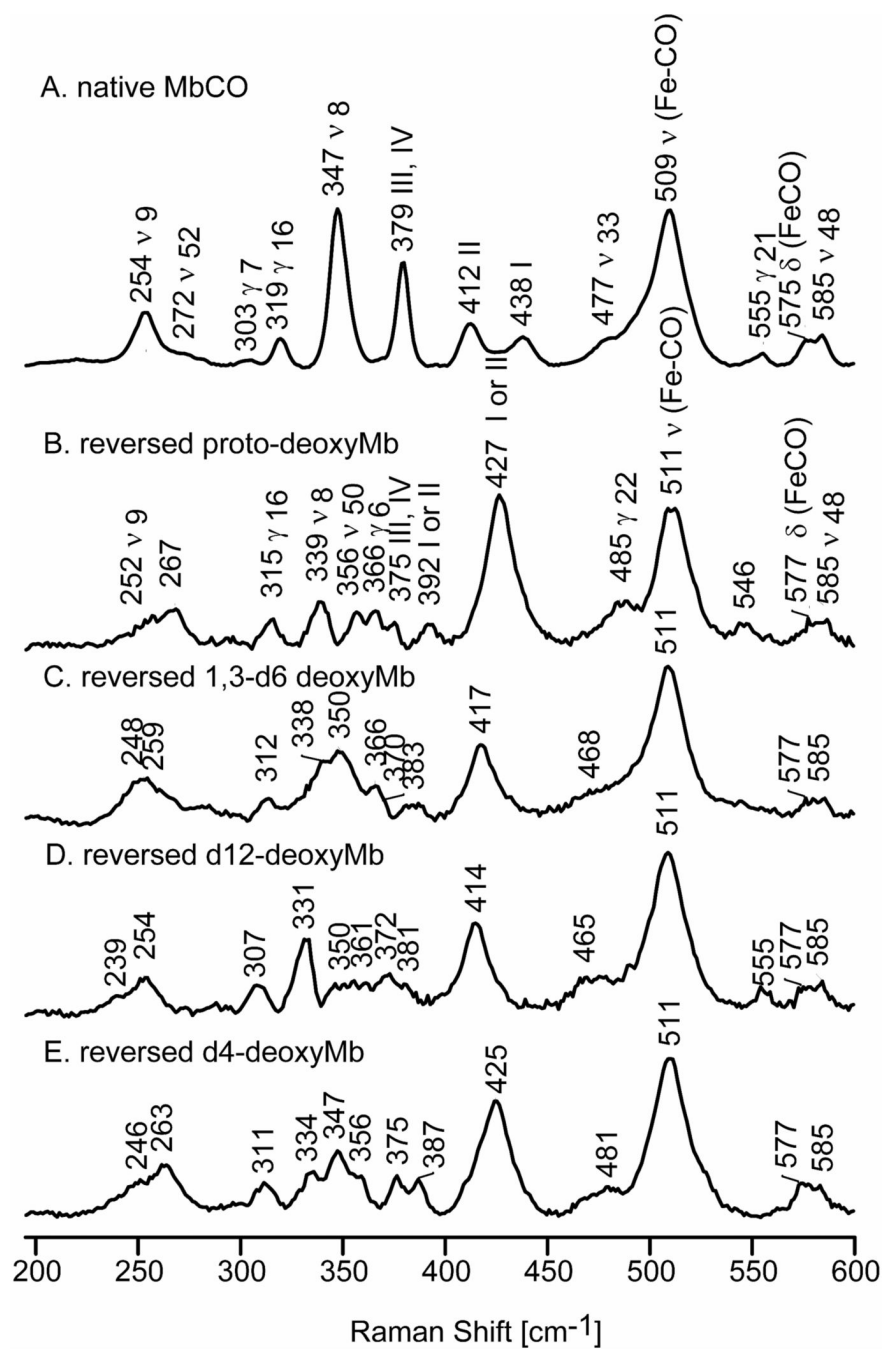


Figure 5. Low frequency RR spectra of native MbCO, (A); reversed proto-MbCO, (B); reversed 1,3-d6-MbCO, (C); reversed d12-MbCO, (D) and reversed d4-MbCO, (E).

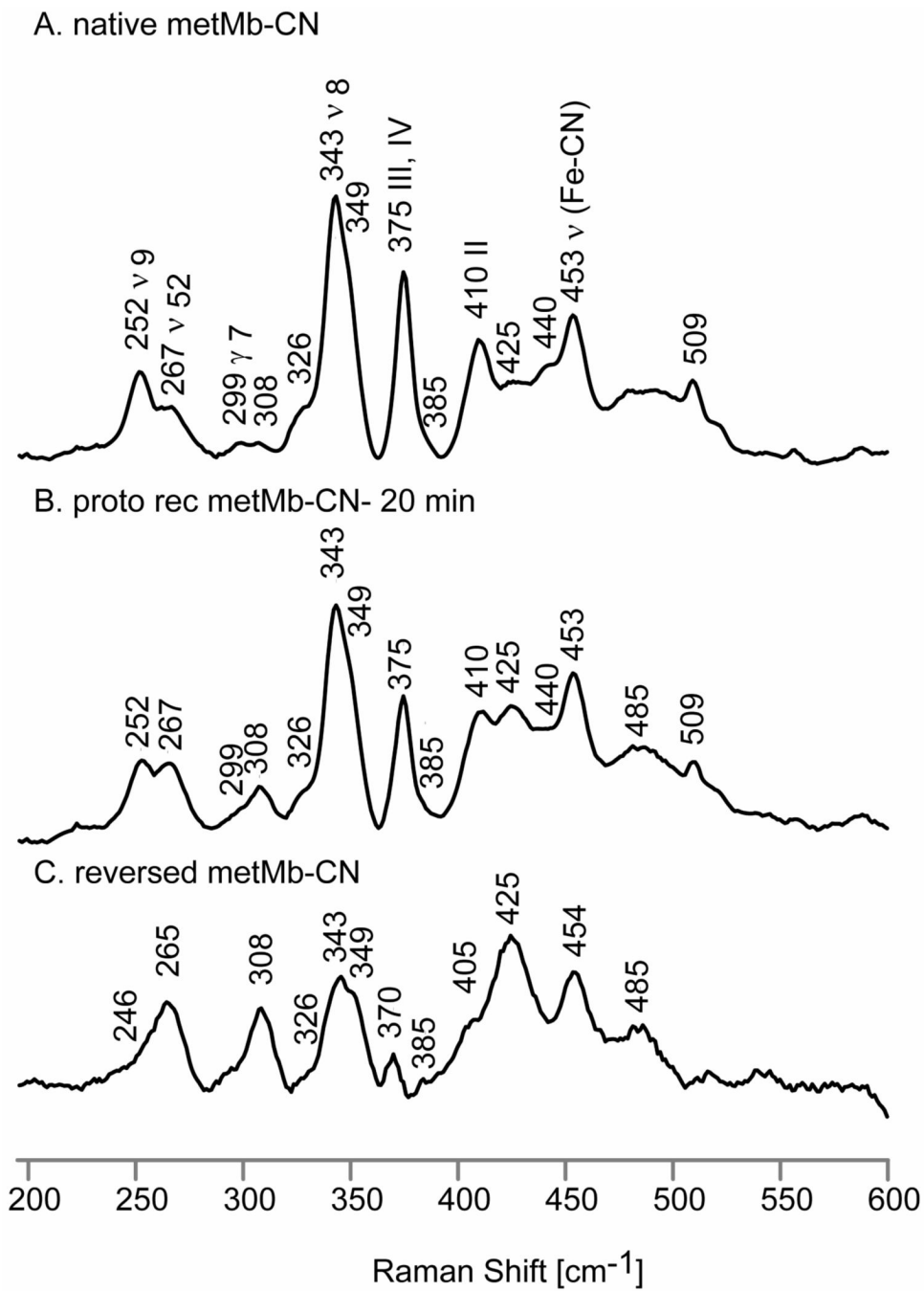


Figure 6. Low frequency RR spectra of native metMb-CN, (A); 20-min reconstituted metMb-CN, (B) and reversed metMb-CN, (C).

Table 1

Summary of observed RR frequencies [cm^{-1}] for native and reversed metMb, deoxyMb, MbCO and metMb-CN together with their isotopic shifts [$\Delta\text{d}1,3\text{-d}6/\Delta\text{d}12/\Delta\text{d}4$].

mode	metMb ^d		deoxyMb		MbCO		metMb-CN	
	native ^d	reversed ^d	native	reversed	native	reversed	native	reversed
$\nu_{(\text{Fe-His})}$			220 [0/0/0]	220 [0/0/0]				
ν_9			240 [2/7/3]		254 [2/7/3]	252 [4/13/6]	252	246
?				251 [11/14/1]		267 [8/13/4]	267	265
ν_{52}	272 [0/1]	272 [0/1]	285 [3/4/1]		272 [0/2/3]			
ν_7	305 [4/5]	307 [1/4]	304 [3/5/6]	298 [2/4/1]	302 [2/3/5]		299	
ν_{16}					319 [2/5/2]	315 [2/8/4]	308	308
ν_6	336 [1/4]	336 [1/4]	335 [1/1/20]	335 [1/1/20]	354 [0/0/19]	366 [0/0/19]		
ν_8	344 [2/3]		343 [2/5/6]	335 [1/9/2]	347 [2/9/0]	339 [1/7/5]	343	343
ν_{50}						356 [6/6/0]		
III,IV	375 [2/9]	366 [2/8]	370 [4/14/2]	360 [2/12/2]	379 [4/15/0]	375 [5/14/0]	375	370
I or II				388 [13/16/4]		392 [9/11/5]		
II	408 [11/12]		405 [14/14/1]		412 [9/11/0]		410	
I or II		422 [9/10]		420 [10/13/3]		427 [10/13/2]		425
I	439 [4/6]		436 [6/8/4]	436 [2/2/3]	438 [7/8/3]		440	
I or II		439 [11/11]						453
$\nu_{(\text{Fe-CN})}$								
ν_{33}	473 [13/16]		487 [7/11/0]		477 [15/19/2]			
ν_{22}	501 [16/18]	482 [10/16]	499 [9/19/8]	480 [18/21/4]		485 [17/20/4]		
$\nu_{(\text{Fe-CO})}$								
ν_{21}	548 [2/9]	548 [2/9]	545 [5/17/10]	545 [2/2/2]	509 [0/0/0]	511 [0/0/0]		
$\delta_{(\text{FeCO})}$					555 [6/18/11]	546 [2/2/2]		
ν_{48}					575 [0/0/0]	577 [0/0/0]		
ν_4	1371 [0/0]	1371 [0/0]	1356 [0/0/1]	1356 [0/0/1]	585 [0/0/0]	585 [0/0/0]		
ν_{12}	1387 [0/0]	1387 [0/0]			1373 [0/0/0]	1373 [0/0/0]		
ν_{29}	1401 [0/0]	1401 [0/0]			1390 [0/0/2]	1390 [0/0/2]		
ν_{28}	1426 [0/0]	1426 [0/0]	1426 [0/0/0]	1426 [0/0/0]	1401 [0/0/2]	1401 [0/0/2]		
					1432 [0/0/0]	1432 [0/0/0]		

mode	metMb ^a		deoxyMb		MbCO		metMb-CN	
	native ^a	reversed ^a	native	reversed	native	reversed	native	reversed
$\delta(=C_0H_2)$	1451 [0/0]	1451 [0/0]	1448 [0/0/6]	1448 [0/0/6]	1470 [6/7/7]	1470 [4/5/4]		
v ₃	1482 [0/0]	1482 [0/0]	1473 [2/2/8]	1473 [2/2/8]	1501 [1/3/10]	1501 [1/3/10]		
v ₃₈	1512 [0/0]	1512 [0/0]	1526 [0/0/16]	1526 [0/0/16]	1546 [1/3/10]	1546 [1/3/10]		
v ₃₈	1521 [0/0]	1521 [0/0]						
v ₁₁	1544 [2/4]	1544 [2/4]	1545 [1/3/16]	1545 [2/3/16]	1563 [4/5/8]	1563 [4/5/8]		
v ₂	1563 [2/4]	1563 [2/4]	1564 [3/4/4]	1564 [3/4/4]	1585 [1/2/5]	1585 [1/2/4]		
v ₃₇	1583 [0/0]	1583 [0/0]	1590 [0/4/4]	1590 [0/3/3]	1607 [0/2/4]	1607 [0/2/4]		
v ₁₀			1607 [0/0/10]	1607 [0/0/10]	1636 [0/0/10]	1636 [0/0/10]		
v _{Ca=Cb}	1620 [0/0]	1620 [0/0]	1618 [0/0/0]	1618 [0/0/0]	1619 [0/0/0]	1619 [0/0/0]		
v _{Ca=Cb}		1630 [0/0]		1632 [0/0/0]		1629 [0/0/0]		

^aFrom ref. 25.